

Numerical Electromagnetic Field Analysis of Transient Magnetic Fields in a Nacelle Caused by a Lightning Stroke to a Wind Turbine Generator System

K. Yamamoto, T. Chikara, A. Ametani

Abstract--The damages caused by lightning are particularly severe in the case of wind turbine generator systems. The nacelle is composed of steel grids covered with GFRP (glass-fiber reinforced plastics) in order to reduce its weight. When lightning strikes a wind turbine generator system, the current thus generated flows into the ground through down conductors in the blades, the steel grids of the nacelle, and the tower. Further, the current flowing near the nacelle produces large magnetic fields inside the nacelle, and the communication and control systems either break down or malfunction. We have analytically and experimentally investigated the transitions of the magnetic fields in the nacelle by using an FDTD (Finite Difference Time Domain) method and a reduced-size model of a wind turbine generator system.

Keywords: wind turbine generator system, lightning protection, FDTD method, transient magnetic fields.

I. INTRODUCTION

In recent years, several accidents have occurred in wind turbine generator systems because of natural disasters such as lightning and typhoons. The damages caused by lightning are particularly severe [1–9].

A wind turbine generator system is composed of blades, a nacelle, a tower, etc. In order to reduce the weight of the blades and the nacelle, the blades have been manufactured using GFRP (glass-fiber reinforced plastics), while the nacelle is composed of steel grids covered with GFRP. When lightning strikes a wind turbine generator system, current is generated. This current flows into the ground primarily through the steel grids of the nacelle. The current flowing near the nacelle produces large magnetic fields inside the nacelle [10]. As a result, the communication and control systems either break down or malfunction [1–3].

In this paper, we have analytically and experimentally investigated the transitions of the magnetic fields in the nacelle. For the analytical studies, an FDTD (Finite Difference Time Domain) method is used [11–15]. A reduced-size model

of a wind turbine generator system is used for the experimental studies [7, 8].

II. REDUCED-SIZE EXPERIMENTS AND FDTD SIMULATIONS

A. Reduced-Size Model

Experiments using an actual wind turbine generator system have many restrictions. Therefore, a reduced-size model, as shown in Fig. 1, has been used in this study. We wanted to develop a 6/100-scale model of an actual wind turbine generator system that has 40-m-long blades and a 60-m-high tower. Therefore, in the reduced-size model, the length of the blades and the height of the tower should have been 2.4 m and 3.6 m, respectively. However, because of the restrictions on experimental space, we use a model with 1.5-m-long blades and a 1.5-m-high tower. This configuration does not influence the magnetic fields in the nacelle, because we have used the experimental results at a time before the traveling wave reached the nacelle again from the tip of the blade and the root of the tower after initially arriving at the nacelle. The results at 6 ns shown in this paper are equivalent to those at 0.1 μ s in an actual scale because of the scale ratio of 6/100.

The blades are made of vinyl chloride, and an insulated copper wire (cross-sectional area: 2 mm²) is traced on each blade in order to represent a lightning conductor. The actual tower is tapered; however, the tower of the scale model is tubular with an outer diameter of 20 cm and a thickness of 3 mm.

An enlarged view of the nacelle is shown in Fig. 2. The down conductors in the blades and the nacelle are usually connected by a brush or a small gap. Therefore, the down conductors and the nacelle are directly connected in the reduced-size model. The nacelle of a recent large-scaled wind turbine generator system is often manufactured by using steel grids covered with GFRP. In these experiments, the nacelle model using steel grids shown in Fig. 2 is used for measuring the transient magnetic fields in it. The bottom face of the nacelle is a steel plate; however, there is a hole at the junction of the tower and the nacelle.

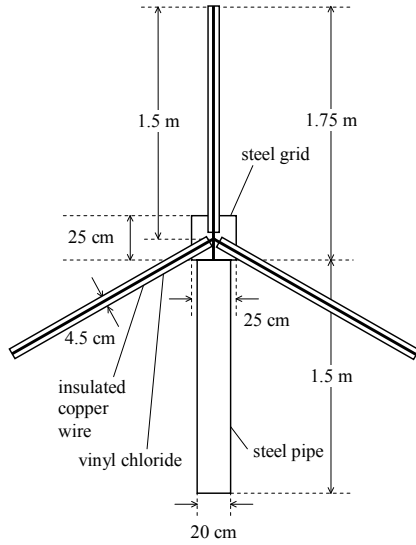
B. Measuring Instrument

The oscilloscope used in the study is TDS784D (Tektronix); it has a bandwidth of DC~1 GHz. The current sensor used is CT-1 (Tektronix); its bandwidth is 25 kHz~1.5 GHz.

K. Yamamoto is with Kobe City College of Technology, Kobe Hyogo 651-2194, Japan (e-mail and phone/fax number of corresponding author: kyamamoto@mem.iee.or.jp, +81-78-795-3239, respectively).

T. Chikara is with Doshisha University, Kyo-tanabe Kyoto 610-0321, Japan (e-mail of corresponding author: dti0103@mail4.doshisha.ac.jp).

A. Ametani is with Doshisha University, Kyo-tanabe Kyoto 610-0321, Japan (e-mail of corresponding author: aametani@mail.doshisha.ac.jp).

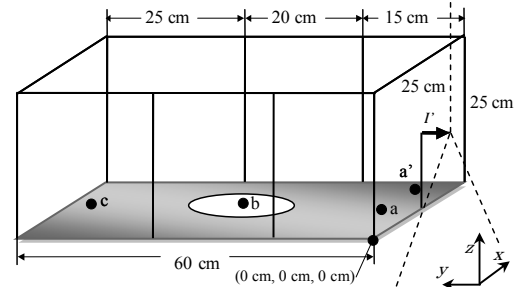


(a) Dimensions of the reduced-size model



(b) Picture of the reduced-size model

Fig. 1 Reduced-size model of a wind turbine generator system



(a) Dimensions of the nacelle model



(b) Picture of the nacelle model

Fig. 2 Enlarged view of the nacelle

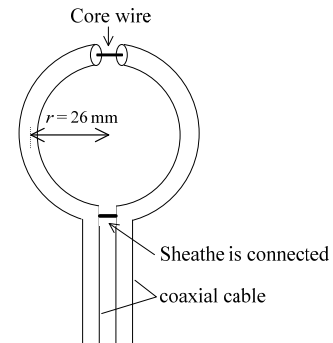


Fig. 3 Transient magnetic field sensor

The transient magnetic sensor is self-produced. Fig. 3 shows the configuration of the one-turn-coil sensor. This sensor gives as its output the induced voltage generated by the flux change through the one-turn coil. Integration of the induced voltage gives the average magnetic field at the place at which the sensor is set up. The maximum error of this sensor has been proved to be 15% [16].

C. Experimental Conditions

The reduced-size model is set up as shown in Fig. 4. An aluminum plate (5 m \times 5 m) is embedded and grounded. The pulse generator used is INS-4040 (NoiseKen); it charges a coaxial cable and discharge by using a mercury relay and can give as its output a current with a steep rise time of several ns. The current generated by the pulse generator is injected by using a 480- Ω resistor R_i from a current lead wire of a coaxial cable into the reduced-size model. The internal resistance of the pulse generator is 50 Ω , and the surge impedance of the

insulated copper wire used as the current lead wire is approximately 500 Ω [17, 18]. Therefore, the total surge impedance of the lightning channel is (480 + 50 + 500) Ω , which is approximately 1 k Ω [19].

It is observed that lightning mostly strikes the tip of the blade and the rear portion of the nacelle where an observation system of the wind speed and direction is set up [1–3]. These two points are employed as the assumed points of the lightning strokes, as shown in Fig. 4.

The return stroke of most lightning propagates from the wind turbine generation system to the cloud. Here, the current is injected into the coaxial cable from the pulse generator and is led to the lightning-stroke point. The current is injected into the reduced-size model of a wind turbine generation system through R_i . While the current propagates on the current lead wire of the coaxial cable, an electromagnetic field exists inside the coaxial cable and not around the cable. After the current arrives at the lightning stroke point, the current I is

injected into the lightning stroke point, and the current $-I$ is reflected on the sheath of the coaxial cable. This current represents the return stroke propagating from the wind turbine generation system to the cloud [7, 8].

D. Analytical Conditions

The analytical spaces used in this study are shown in Fig. 5. Fig. 5 (a) illustrates the case of a lightning stroke at the tip of the blade and Fig. 5 (b), the case of a lightning stroke at the rear portion of the nacelle. Fig. 5 is an FDTD simulation model of Fig. 4.

The diameter and the length of the tower model are 20 cm and 1.5 m, respectively; the diameter and the length of the down conductor in the blades are 0.8 mm and 1.5 m, respectively. The nacelle is modeled as a 25 cm \times 25 cm \times 60 cm rectangular parallelepiped object. The dimensions of the analytical space are 6 m \times 4 m \times 6 m; this space is divided

into 2.5-cm cubic cells. Liao's second boundary condition is utilized on the six planes surrounding the analytical space in order to model open space. The lightning path and the down conductors in the blades are represented by a thin-wire model [14]. The down conductors are represented by an inclined thin-wire model [15]. The cross section of the tower model is a circle of diameter 20 cm; the cross section is modeled as a step-like surface.

A current is injected through a resistance of $480 + 50 = 530 \Omega$ at the point where lightning is assumed to strike.

E. Comparisons

Fig. 6 shows the injected current in the experiments and simulations. The rise time and the peak value are approximately 2 ns and 1 A, respectively. The output points of the magnetic fields are a (10 cm, 5 cm, 5 cm), a' (15 cm, 5 cm,

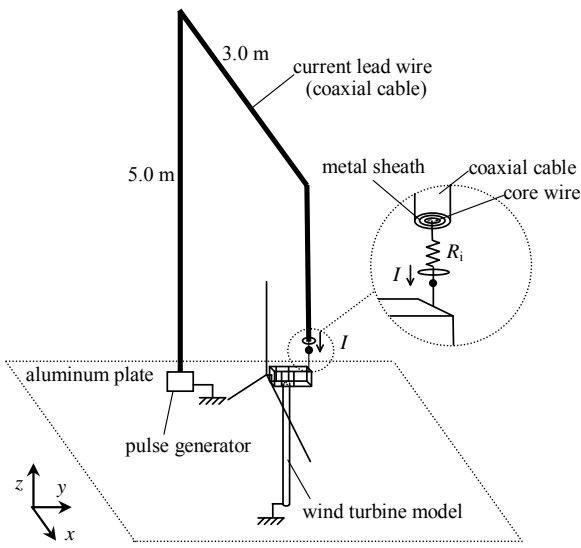
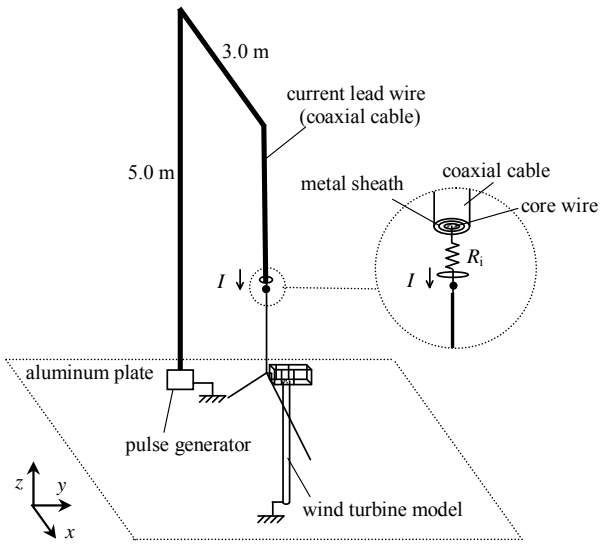


Fig. 4 Experimental setup

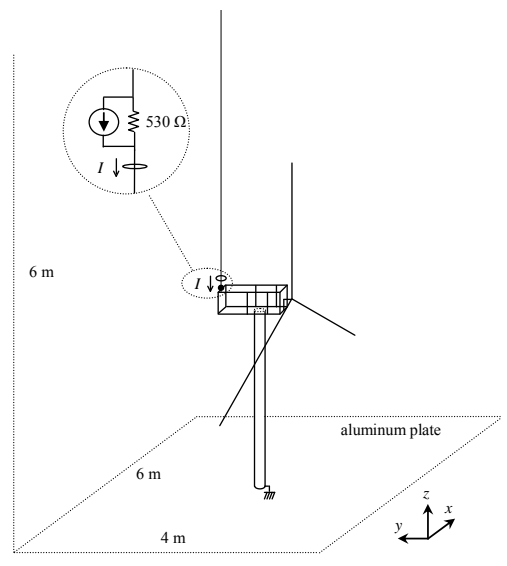
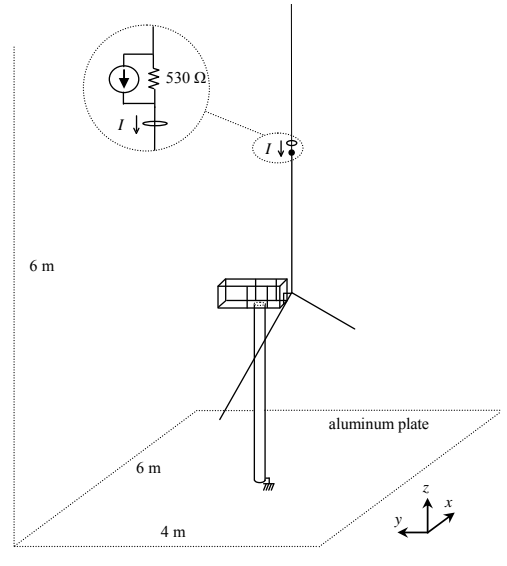
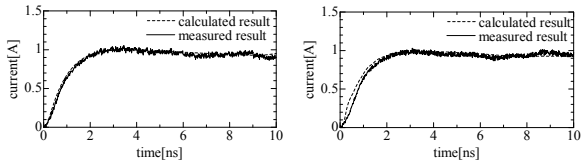
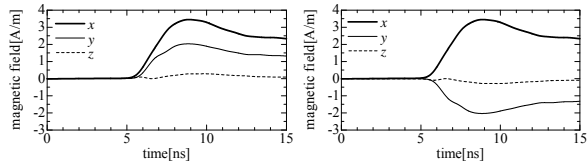


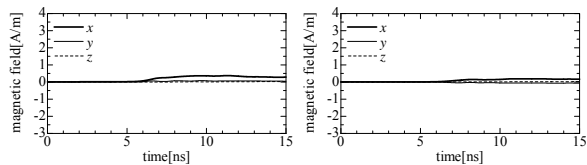
Fig. 5 Analytical setup



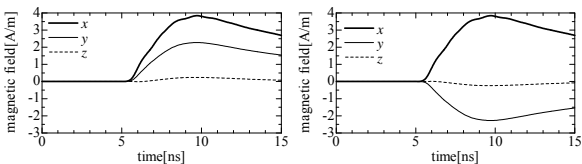
(a) Current into the blade (b) Current into the nacelle
Fig. 6 Injected current waveforms



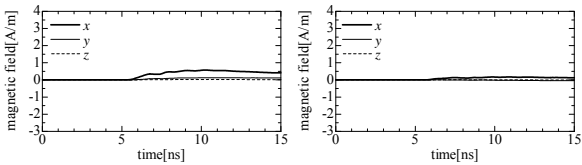
(a) Magnetic field at point a (b) Magnetic field at point a'



(c) Magnetic field at point b (d) Magnetic field at point c
Fig. 7 Measured results of the magnetic fields
(current injected into the tip of the blade)



(a) Magnetic field at point a (b) Magnetic field at point a'

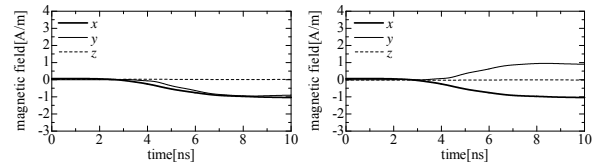


(c) Magnetic field at point b (d) Magnetic field at point c

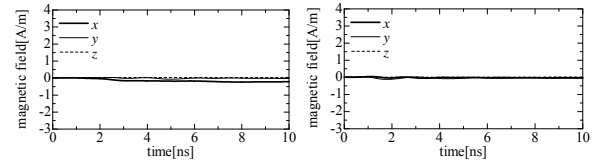
Fig. 8 Calculated results of the magnetic fields
(current injected into the tip of the blade)

5 cm), b (10 cm, 30 cm, 5 cm), and c (10 cm, 55 cm, 5 cm), as shown in Fig. 2. At each point, the magnetic fields along the x , y , and z directions are shown in Figs. 7–10. Points a and a' are typical at the front of the nacelle, symmetrical. Points b and c are typical at the center and rear of the nacelle. The calculated results agree well with the measured results, and the maximum error is approximately 15%. The error arises from measurements and calculations; it can be guessed that the main error arises from the accuracy of the self-produced magnetic sensor.

Fig. 7 shows the case of a lightning stroke at the tip of the blade. Points a and a' are symmetrical. The magnitude and the polarity of the magnetic fields along the x direction at these points are equal, as shown in Figs. 8 (a) and (b). The magnetic fields in the y direction are equal in magnitude but opposite in polarity. The magnetic fields along the z direction are far smaller than those along other directions. The waveforms of

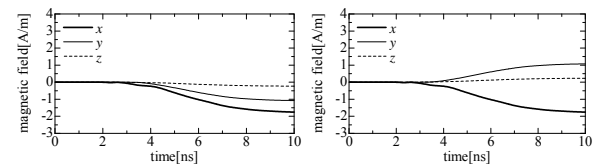


(a) Magnetic field at point a (b) Magnetic field at point a'

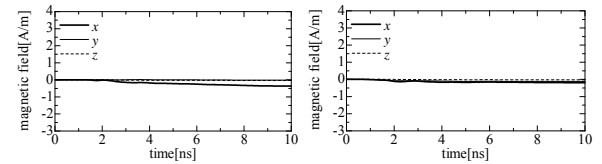


(c) Magnetic field at point b (d) Magnetic field at point c

Fig. 9 Measured results of the magnetic fields
(current injected into the rear portion of the nacelle)

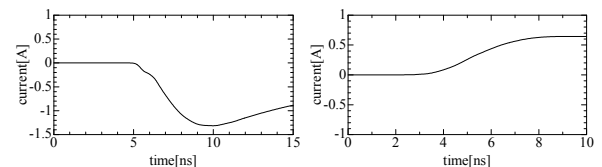


(a) Magnetic field at point a (b) Magnetic field at point a'



(c) Magnetic field at point b (d) Magnetic field at point c

Fig. 10 Calculated results of the magnetic fields
(current injected into the rear portion of the nacelle)



(a) Current into the blade (b) Current into the nacelle

Fig. 11 Current waveform I

the magnetic fields at points b and c are shown in Figs. 8 (c) and (d), respectively. It is observed that the magnetic fields at points b and c are smaller than those at point a. From the above results, it is evident that the current flowing through the down conductor of the blades exerts a greater influence on the magnetic fields inside the nacelle than the current flowing in the grids of the nacelle.

Figs. 9 and 10 show the case when lightning strikes at the rear portion of the nacelle. It should be noted that the magnetic fields at the front of the nacelle are larger than those in the rear irrespective of the point of injection of the lightning current. This phenomenon can be explained as follows. The surge impedance of each down conductor is larger than that of the tower. However, as the three down conductors are spread radially, the total surge impedance is small. Therefore, a comparatively large current flows into the down conductors, as shown in Fig. 11; thus, it is evident that the current flowing

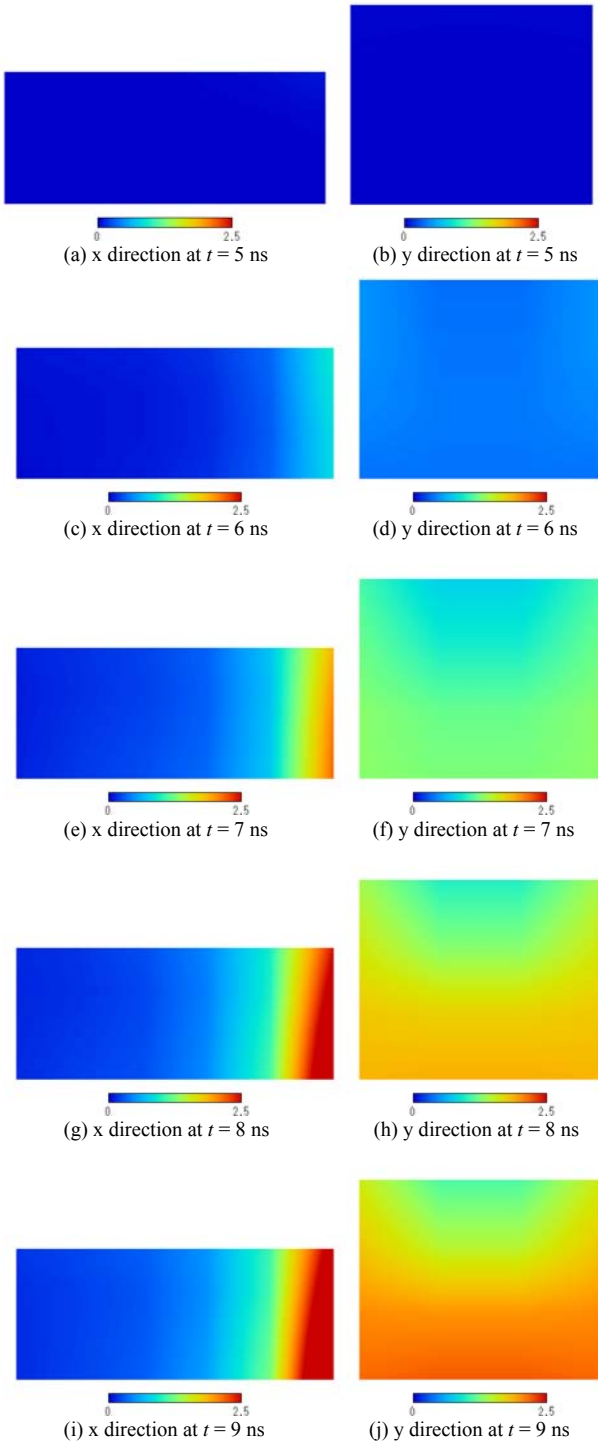


Fig. 12 Transitions of the magnetic fields [A/m]
(current injected into the tip of the blade)

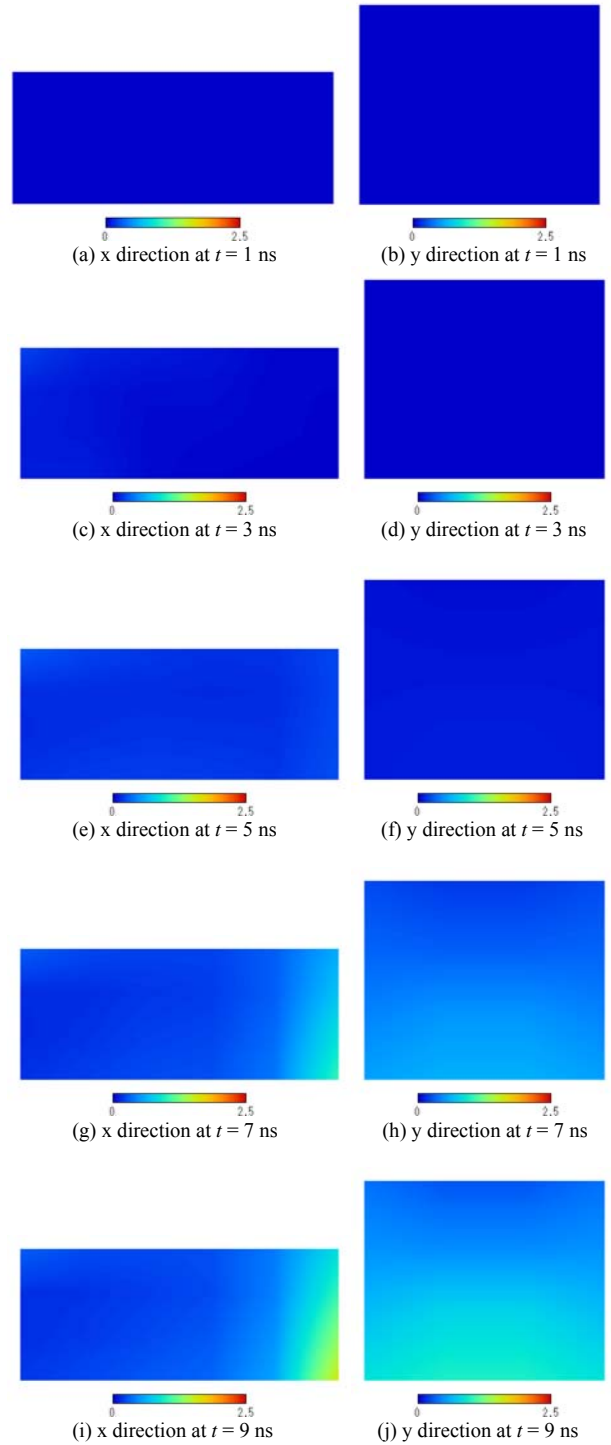


Fig. 13 Transitions of the magnetic fields [A/m]
(lightning to the rear portion of the nacelle)

through the down conductors of the blades influences the magnetic fields.

Fig. 12 shows the transitions of the magnetic fields in the y direction on the zx plane at $y = 5$ cm, and the transitions of the magnetic fields in the x direction on the yz plane at $x = 10$ cm when the current is injected into the tip of the blade. Fig. 13 shows the calculated result when the current is injected into the rear portion of the nacelle. From these results, it is obvious

that the magnetic fields at the front of the nacelle are larger than those in the rear regardless of the point of injection of the lightning current.

III. PROPOSAL TO DECREASE MAGNETIC FIELDS IN A NACELLE

In the previous section, we discussed that the large magnetic fields around the front portion of the nacelle are generated by the current flowing in the down conductors of

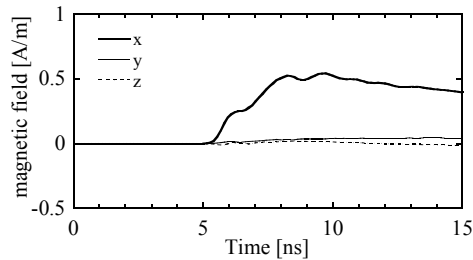


Fig. 14 Calculated results of the magnetic fields at point a with a conductor plate at the front of the nacelle (current injected into the tip of the blade)

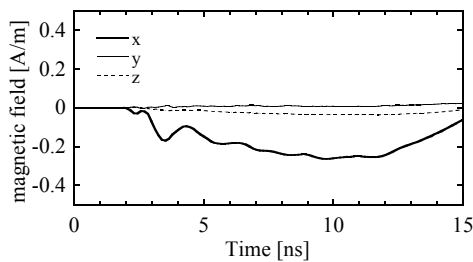


Fig. 15 Calculated results of the magnetic fields at point a with a conductor plate at the front of the nacelle (current injected into the rear portion of the nacelle)

the blades. In order to decrease the large magnetic fields, we propose that the front of the nacelle be covered with a conductor plate or mesh. This conductor plate or mesh will shield the front of the nacelle from the electromagnetic fields caused by the current in the down conductors. The calculated results are shown in Figs. 14 and 15.

It can be confirmed that the conductor plate in the front portion is effective in decreasing the magnetic fields in the nacelle; the magnetic fields as shown in Figs. 14 and 15 can decrease by 4%~16% in comparison with the fields shown Figs. 8 (a) and 10 (a).

IV. CONCLUSIONS

The magnetic fields in a nacelle due to lightning strikes at the tip of the blade and the rear portion of the nacelle have been studied experimentally and analytically. For the analytical studies, the FDTD (Finite Difference Time Domain) method is used. The reduced-size model of a wind turbine generator system is used for the experimental studies. The calculated results agree well with the measured results.

It was observed that the magnetic fields at the front of the nacelle are larger than those at the rear of the nacelle regardless of the points of injection of the lightning current. The lightning current flowing through the down conductor in the blades has a strong influence on the magnetic fields in the nacelle. Hence, we have proposed that the front of the nacelle be covered with a conductor plate or a mesh in order to decrease the large magnetic fields and have proved the effectiveness of using such a plate or mesh by the FDTD method.

V. REFERENCES

- [1] NEDO, "Wind Turbine Failures and Troubles Investigating Committee Annual Report," (2005) (in Japanese).
- [2] NEDO, "Wind Turbine Failures and Troubles Investigating Committee Annual Report," (2006) (in Japanese).
- [3] NEDO, "Wind Turbine Failures and Troubles Investigating Committee Annual Report," (2007) (in Japanese).
- [4] IEC TR 61400-24, "Wind turbine generator systems-Part24 : Lightning protection" (2002).
- [5] T. Soerenson, M. H. Brask, P. Grabau, K. Olsen, and M. L. Olesen, "Lightning damages to power generating wind turbines," International Conference on Lightning Protection, pp. 1-6, Birmingham, UK (1998)
- [6] I. Cotton, B. Mcniff, T. Soerenson, W. Zischank, P. Christiansen, M. Hoppe-Kilpper, S. Ramakers, P. Pettersson, and E. Muljadi, "Lightning protection for wind turbines," International Conference on Lightning Protection, Rhodes, Greece, pp. 848-853 (2000).
- [7] K. Yamamoto, T. Noda, S. Yokoyama and A. Ametani, "An experimental study of lightning overvoltages in wind turbine generation systems using a reduced-size model," Electrical Engineering in Japan, vol. 158, no. 4, pp. 22-30 (2007-3).
- [8] K. Yamamoto, T. Noda, S. Yokoyama, and A. Ametani, "Experimental and Analytical Studies of Lightning Overvoltages in Wind Turbine Generator Systems," Electric Power Systems Research (2008-10).
- [9] K. Yamamoto, T. Noda, S. Yokoyama, and A. Ametani, "Grounding Characteristics of a Wind Turbine Generation System and Voltage Rise around It," International Conference on Grounding and Earthing (Ground2006), pp.415-419, Maceio, Brazil (2006-11).
- [10] K. Yamamoto, T. Chikara, T. Senoh, and A. Ametani, "Magnetic Fields in the Nacelle of a Wind Turbine Generator System Due to Lightning Strikes," International Conference on Lightning Protection (ICLP), 5c-3, Uppsala, Sweden (2008-6).
- [11] K. S. Yee, J. S. Chen, and A. H. Chang, "Conformal finite-difference time-domain (FDTD) with overlapping grids," IEEE Trans. Antennas Propag., vol. 40, pp. 1068-1075 (1992)
- [12] Karl S. Kunz and Raymond J. Luebbers, "The Finite Difference Time Domain Method for Electromagnetics," Boca Raton, FL, CRC Press (1993).
- [13] R. Yonezawa, K. Miyajima, T. Noda, S. Yokoyama, and Y. Takahashi, "Measurement of magnetic field distribution inside 3-D structure due to lightning current and its FDTD simulation," Proc. of the IWHV (International Workshop on High Voltage Engineering) 2003, ED-03-38, SP-03-27, HV-03-27 (2003).
- [14] T. Noda and S. Yokoyama, "Thin wire representation in finite difference time domain surge simulation," IEEE Trans. Power Delivery, vol. 17, no. 3, pp. 840-847 (2002-7).
- [15] T. Noda, R. Yonezawa, S. Yokoyama, and Y. Takahashi, "Error in propagation velocity due to staircase approximation of an inclined thin wire in FDTD surge simulation," IEEE Trans. Power Delivery, vol. 19, no. 4, pp. 1913-1918 (2004-10).
- [16] J. G. Anderson and J. H. Hagenguth, "Magnetic Fields around a Transmission Line Tower," Power Apparatus and Systems, Part III. Transactions of the American Institute of Electrical Engineers, vol. 77, Issue 3, pp. 1644-1649 (1958-4).
- [17] T. Hara, O. Yamamoto, M. Hayashi, and C. Uenosono, "Empirical formulas of surge impedance for single and multiple vertical cylinder," IEEEJ Trans., PE, vol. 110, no. 2, pp. 129-137 (1990-2) (in Japanese).
- [18] A. Ametani, Y. Kasai, J. Sawada, A. Mochizuki, and T. Yamada, "Frequency-dependent Impedance of Vertical Conductors and a Multiconductor Tower Model," IEE Proc. Gener. Transm. Distrib., vol. 141, No. 4 (1994-7).
- [19] Investigating R&D Committee on Lightning Parameters for Insulation and Protection Designs of Power Systems, "Lightning Parameters for Insulation and Protection Designs of Power Systems," Technical Report of IEEEJ, No. 1033 (2005-9) (in Japanese).